A Deeper Analysis of Cataclysmic Variable V383 Vel

Catherine M. Slaughter[1] and Samuel J. Drew[1]

[1]*Department of Physics and Astronomy, Dartmouth College, Hanover, NH*

ABSTRACT

V383 Vel is a dwarf nova type cataclysmic variable star system. Originally discovered in 1938 and identified as a CV in 2000, it has gone largely unstudied in recent years. Using data taken on SAAO's 74-in telescope, this paper aims to determine some of the characteristics of the system, particularly the orbital period and radial velocity. In doing so, we find a period of $0.253 \pm .0057$ days. The radial velocity of the system could not be measured, implying that the secondary in the system is significantly more dim than the white dwarf.

1. INTRODUCTION

V383 Velorum (V383 Vel) is a dwarf nova that was first identified as a suspected variable star in 1938 during the Bruce Proper Motion Survey of the southern sky (Luyten 1938). For decades, no further observations were made until Williams (2000) investigated the star on Harvard photographic plates and revealed V383 Vel to be a previously unrecognized dwarf nova. Williams improved the star's known position to RA 10h 19m 40.6s, Dec -49°34'15" and known magnitude to lie between 12.5-17. He also determined the star to have a characteristic outburst cycle between 52-60 days and published the object's first finding chart. Since Williams, however, no strong efforts have been made to follow up on the study of V383 Vel, besides brief mentions in a few variable star catalogs (Downes et al. (2001), Kazarovets et al. (2001), Burlak & Henden (2008)). Pretorius & Knigge (2008) did attempt to measure a period for V383 Vel, but was unable to because the system went into outburst during observations. We sought out with the intention of discovering more about this dwarf nova, particularly with respect to its radial velocity and orbital period.

2. OBSERVATIONS AND DATA

2.1. *Instrumentation*

The data used for this paper was taken with SAAO's 74-inch telescope at their site in Sutherland, South Africa.[1] The telescope has a number of instruments that can be used, and the spectral data for this project was taken with a spectrograph called SpUpNIC. SpUpNIC is the end product of the Cassegrain Spectrograph Upgrade project completed in 2015 (Crause et al. 2016). SpUpNIC boasts 9 different diffraction gratings, for this project, grating 6 was used.[2] The specifications for this grating can be found in Table 1.

	Lines/mm	Range (Angstroms)	Dispersion (Angstroms/pixel)
6	600	2800	1.36

Table 1. The specifications for grating number 6 on SpUpNIC[2]

This data was taken in the range of 4200-6700 angstroms, with a slit length of 1.2 arcsec. There are also some filter options available with SpUpNIC, however none were used for this data collection.

Along with the science frames, CuAr frames were taken in a number of telescope positions in order to account for the spectrograph flexure.

An extensive journal of observations used for this paper can be found in Table 6.

2.2. *Reduction Methods*

The pre-processing for this reduction included a number of different steps. First, the data were bias subtracted and flat fielded, and the extreme ends of the spectra were cut off. The proper barycentric Julian dates and velocity correc-

[1] https://www.saao.ac.za/science/facilities/telescopes/1-9m/

[2] https://www.saao.ac.za/science/facilities/instruments/spupnic-spectrograph-upgrade-newly-improved-cassegrain/

tions are calculated and written into the headers. Finally, science exposures were paired up with their corresponding arc exposures, based on telescope position. This data is printed into a file to be used in IRAF's REFSPEC task later.

Once the pre-processing is done, 1D spectra can be extracted from the images. First, standard IRAF tasks are implemented in order to align the spectra properly.

The data are extracted using a task which implements the optimal extraction process outlined in Horne (1986). This task will typically fail for 2-3 frames a night, and failed frames are rerun with IRAF's built-in tasks

Once the object files have been extracted, the same needs to be done for the arc spectra. The python script used for this takes in the list of science-arc image pairs, in order to extract the spectrum from the same part of the chip as the science frame. Finally, standard IRAF tasks are used to propagate the wavelength solutions for the arc spectra to their corresponding object spectra.

Once the data is fully reduced, the reduced spectra were splotted and examined. Two spectra, da991278 and da991424, were determined to be unusable. The first showed no spectral features at all and was probably taken through clouds, the second was especially messy in the blue portion of the spectrum, so much so that the $H\beta$ line could not be found.

A flux-calibrated combined spectrum of all the good data taken can be found below.

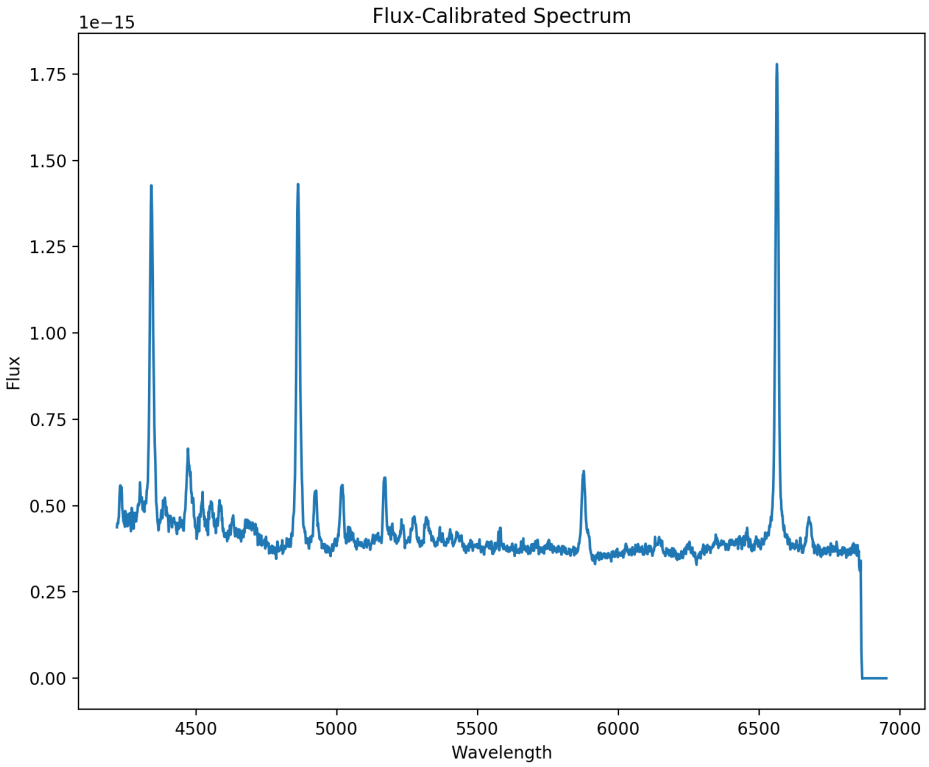

Figure 1. A combined and flux-calibrated spectrum of V383 Vel.

3. ANALYSIS METHODS

3.1. *Measuring Emission Lines by Convolution*

The first step for measuring radial velocities is to convolve the line profile with an asymmetric function. A python task written for this is based on the process originally outlined in Schneider & Young (1980). This task was run on both the $H\alpha$ and $H\beta$ lines of the spectra. A derivative of a Gaussian optimized for the FWHM of the lines (12

Angstroms) was chosen as the convolution function. The output of the task is a time series file that will be used to find the orbital period.

3.2. *Determining Orbital Period with Sine Search*

Once the time series files are collected, the period of the system is determined. This is done with a task written for the purpose of finding cataclysmic binary orbital periods, and works by searching for sin functions to fit unevenly sampled data. The data for this and any ground-based observational paper will be unevenly sampled due to the rotation of the Earth. Each time series file (the $H\alpha$ and $H\beta$) was run through the task, looking for fits with frequencies between 0.1 and 20 cycles per day. These fits are found in the form of

$$v(t) = \gamma + K \sin(2\pi(t - T_0)/P) \tag{1}$$

A periodogram is made for the data, with the top three most likely fits labeled. Reviewing the best fit set for each line gives the following parameters.

Line	T_0	Period	K-Vel	γ
$H\alpha$	58538.2792	.2559630	46.54	53.92
$H\beta$	58538.3181	.2474987	73.52	125.95

Table 2. The top fit set for the $H\alpha$ and $H\beta$ time series data.

While the periods of these fits appear to be different, the uncertainties shown in tables 3 and 4 show that they are consistent within their mutual uncertainties.

The first sets are plotted along with the original time series data sets below. Note that the x-axes on these graphs are in terms of phase, not Julian Date.

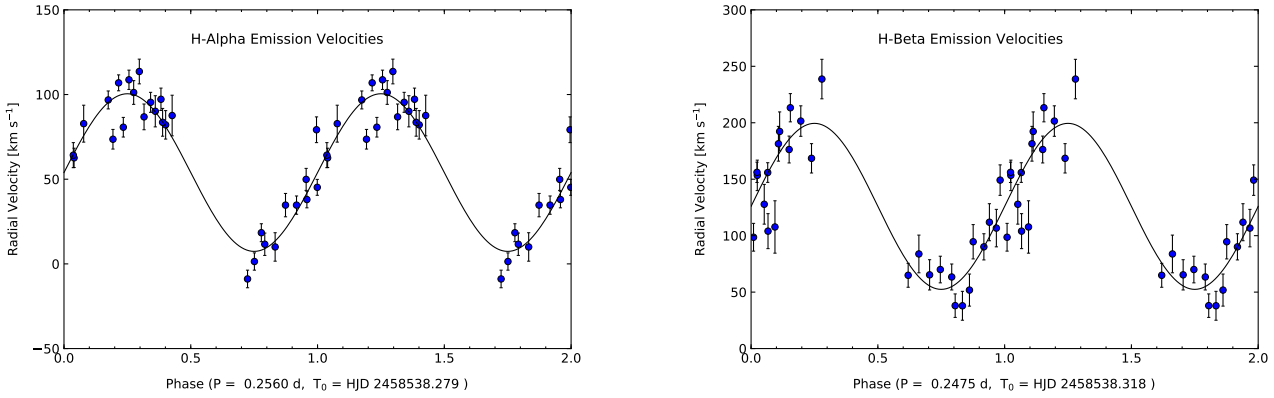

Figure 2.

In the case of this data, the first and second best aliases are very close on the periodiagram, which means that a Monte Carlo alias test (as outlined in Thorstensen & Freed (1985)) can be used to find the errors in the fit measurements. The Monte Carlo simulation was run using the second best fit as the "true" fit, because the scatter in the expected noise is greater, so a larger region will be sampled. A simulation of 10,000 trials was run. The errors output by the Monte Carlo are as follows. The true parameters were chosen 9812 times for the $H\alpha$ data, and 9647 times for $H\beta$.

Value	σ
T_0	0.00473406
Period	0.00713995
K-Vel	4.70708338
γ	3.77994808

Table 3. $H\alpha$ Monte Carlo output uncertainties.

Value	σ
T_0	0.00979001
Period	0.00978989
K-Vel	8.85688938
γ	8.77927042

Table 4. $H\beta$ Monte Carlo output uncertainties.

From here, the data from the two emission lines' data are combined using a weighted average. This average is calculated using the best fits from the initial sin curve fitting and the uncertainties from the Monte Carlo simulation. The final values for the combined fit, along with a plot of the fit, can be found below.

	Mean	σ
T_0	58538.2	0.0042619
Period	0.253024	0.0057687
K-Vel	52.4821	4.1565
γ	65.1844	3.4718

Table 5. Average values and uncertainties for the best fits of the data.

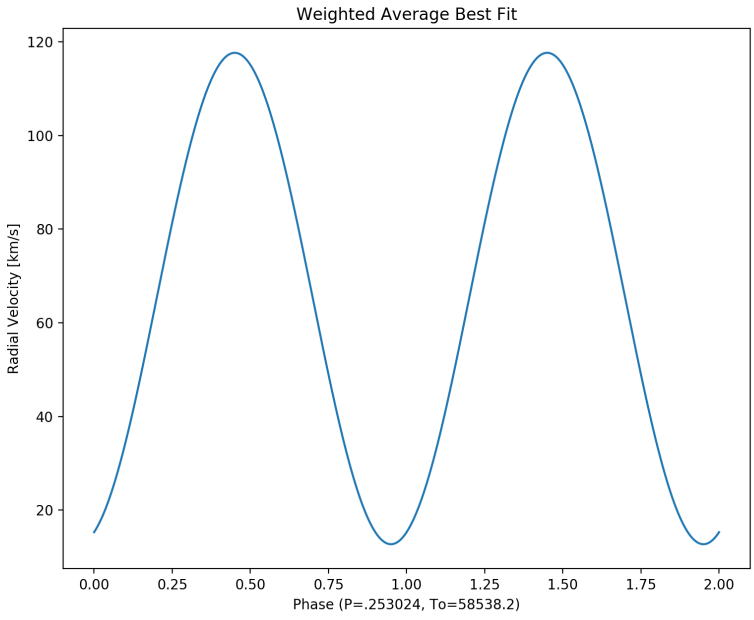

Figure 3. The final, weighted average fit

3.3. *Searching for Absorption Features of the Secondary with Cross-Correlation*

While it is possible to find radial velocity with the emission features of the spectra, it would be much more accurate to do so using absorption features. Any absorption lines on these spectra will be due to the secondary star's absorbing light from the primary. In order to look for these features and find an absorption radial velocity, a cross-correlation process (as described in Tonry & Davis (1979)) is used. In this case, the data will be cross-correlated with a composite of some 76 spectra from near K-class stars, shifted as if it has a 0 radial velocity.

In order to perform cross-correlation, however, the spectra are first cleaned of any significant glitches. This can be done simply using splot functionality.

Unfortunately, the cross-correlation fails on every single one of the spectra used. An example output window from a representative spectrum can be found below.

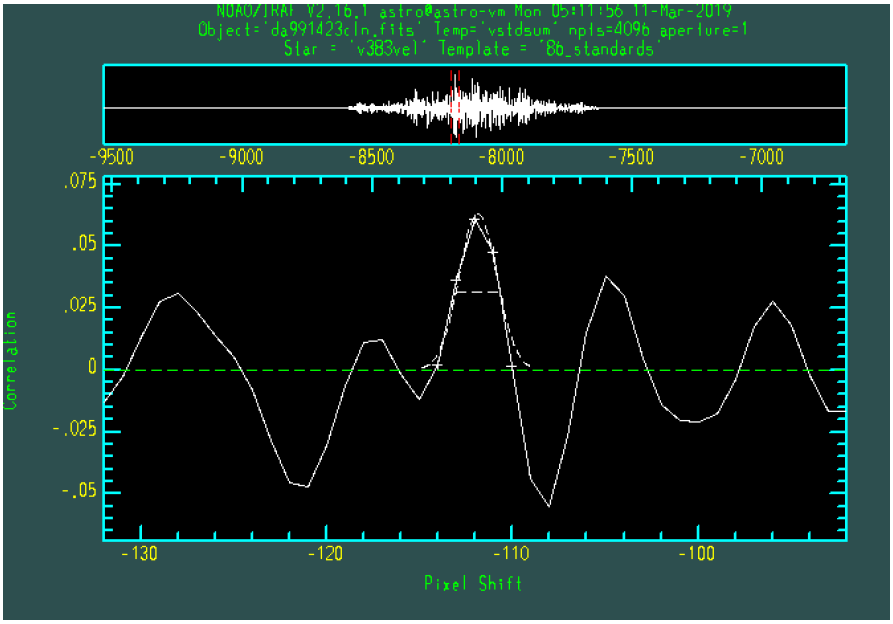

Figure 4. A representative output from the fxcor task.

Most notably, a successful output would have a single strong peak near 0 on the upper graph, which is clearly not the case. While this is indicative of a failed cross-correlation, it is not indicative of bad data. In fact, this failure indicates that the absorption features on this spectrum are so small, they cannot be properly picked out by the cross-correlation. Simply put, the secondary of V383 Vel is too dim to show a significant absorption spectrum. Not the original intended result, but an interesting one nonetheless.

While the absorption features were too small to determine a radial velocity, a guess at the spectral type of the secondary can be made by looking at the combined, flux-calibrated spectrum in Fig.1. By comparing this spectrum to those found in Jacoby et al. (1984), the absorption features seen on the combined spectrum seem to line up best with an M-Type star. TiO features seem to be particularly strong.

4. CONCLUSIONS

The analysis in this paper shows that the period of V383 Vel is $0.253 \pm .0057$. Unfortunately, the absorption features from the secondary were not strong enough to determine a radial velocity for the system, indicating that the secondary is very dim compared to the white dwarf. By combining and flux-calibrated the data, however, enough absorption features were visible to estimate the secondary's spectral class as a roughly M-class star.

File no.	Date	Time(UT)	Airmass	Exposure Time (s)
1205	2019-02-18	01:37:30	1.1867	1200.0
1206	2019-02-18	01:57:34	1.2315	1200.0
1278	2019-02-20	21:35:08	1.0877	1000.0
1359	2019-02-23	01:15:50	1.1827	900.0
1360	2019-02-23	01:30:54	1.2149	900.0
1361	2019-02-23	01:45:58	1.2514	900.0
1362	2019-02-23	02:01:02	1.2939	900.0
1364	2019-02-23	02:17:23	1.3456	900.0
1365	2019-02-23	02:32:27	1.4005	900.0
1385	2019-02-23	19:34:43	1.2893	900.0
1386	2019-02-23	19:49:47	1.2480	900.0
1387	2019-02-23	20:04:51	1.2116	900.0
1388	2019-02-23	20:19:54	1.1797	900.0
1390	2019-02-23	20:36:17	1.1499	900.0
1391	2019-02-23	20:51:21	1.1265	900.0
1401	2019-02-23	23:07:11	1.0509	900.0
1402	2019-02-23	23:22:15	1.0561	900.0
1403	2019-02-23	23:37:19	1.0639	900.0
1404	2019-02-23	23:52:23	1.0745	900.0
1406	2019-02-24	00:08:25	1.0888	900.0
1407	2019-02-24	00:23:29	1.1057	900.0
1408	2019-02-24	00:38:33	1.1256	900.0
1409	2019-02-24	00:53:37	1.1489	900.0
1423	2019-02-24	03:02:19	1.5525	900.0
1424	2019-02-24	03:17:41	1.6375	720.0
1466	2019-02-25	00:56:43	1.1614	900.0
1467	2019-02-25	01:11:46	1.1902	900.0
1468	2019-02-25	01:26:50	1.2237	900.0
1469	2019-02-25	01:41:54	1.2620	900.0

Table 6. Journal of Observations.

REFERENCES

Burlak, M. A., & Henden, A. A. 2008, Astronomy Letters, 34, 241

Crause, L. A., Carter, D., Daniels, A., et al. 2016, in Proc. SPIE, Vol. 9908, Ground-based and Airborne Instrumentation for Astronomy VI, 990827

Downes, R. A., Webbink, R. F., Shara, M. M., et al. 2001, Publications of the Astronomical Society of the Pacific, 113, 764

Horne, K. 1986, PASP, 98, 609

Jacoby, G. H., Hunter, D. A., & Christian, C. A. 1984, ApJS, 56, 257

Kazarovets, E. V., Samus, N. N., & Durlevich, O. V. 2001, Information Bulletin on Variable Stars, 5135, 1

Luyten, W. J. 1938, Publications of the Astronomical Observatory University of Minnesota, 6, 79

Pretorius, M. L., & Knigge, C. 2008, MNRAS, 385, 1485

Schneider, D. P., & Young, P. 1980, ApJ, 238, 946

Thorstensen, J. R., & Freed, I. W. 1985, AJ, 90, 2082

Tonry, J., & Davis, M. 1979, AJ, 84, 1511

Williams, D. B. 2000, Information Bulletin on Variable Stars, 4994